

Cite this: *Phys. Chem. Chem. Phys.*, 2011, **13**, 15442–15447

www.rsc.org/pccp

Characterizing TiO₂(110) surface states by their work function

Andriy Borodin and Michael Reichling

Received 9th December 2010, Accepted 7th July 2011

DOI: 10.1039/c0cp02835e

The unreconstructed TiO₂(110) surface is prepared in well-defined states having different characteristic stoichiometries, namely reduced (*r*-TiO₂, 6 to 9% surface vacancies), hydroxylated (*h*-TiO₂, vacancies filled with OH), oxygen covered (*ox*-TiO₂, oxygen adatoms on a stoichiometric surface) and quasi-stoichiometric (*qs*-TiO₂, a stoichiometric surface with very few defects). The electronic structure and work function of these surfaces and transition states between them are investigated by ultraviolet photoelectron spectroscopy (UPS) and metastable impact electron spectroscopy (MIES). The character of the surface is associated with a specific value of the work function that varies from 4.9 eV for *h*-TiO₂, 5.2 eV for *r*-TiO₂, 5.35 eV for *ox*-TiO₂ to 5.5 eV for *qs*-TiO₂. We establish the method for an unambiguous characterization of TiO₂(110) surface states solely based on the secondary electron emission characteristics. This is facilitated by analysing a weak electron emission below the nominal work function energy. The emission in the low energy cut-off region appears correlated with band gap emission found in UPS spectra and is attributed to localised electron emission through Ti³⁺ (3d) states.

The work function ϕ is a well-established concept in solid state physics to describe the energy needed to remove an electron from a solid and place it at a position where it has only a negligible interaction with the solid. It is insofar the equivalent to the concept of the *ionization potential* established in atomic physics as the work function describes the minimum binding energy and relates the *Fermi energy* E_F in a solid to the *vacuum potential* E_{vac} that is the reference energy of the free electron. It has early been rationalized that the surface that is crossed when removing the electron from the bulk has a significant influence on the value of the work function and for a metal surface, this is usually explained by a surface dipole formed by the electron density due to wave functions extending out of the surface and the net positive charge in a near surface electron depleted region.¹ The work function may significantly be reduced by the presence of adsorbates at the surface where alkali atoms with their low ionization potential are a prominent example for a strong adsorbate effect.² For insulators and semiconductors, surface defects and adsorbates introducing a higher density of band gap states influence the surface dipole structure or act as local escape channels for electrons and,

therefore, play a crucial role in the value of the work function.³ For an adsorbate, the effectiveness in changing the work function is mostly related to the electronegativity of the species under consideration as this determines the ability of the adsorbate for inducing near surface charge accumulation.⁴ Related effects in oxide materials have been reported, for instance, for indium tin oxide where the work function can be controlled by an appropriate selection of the adsorbate.⁵

Titanium dioxide (TiO₂, titania) is a small band gap semiconductor that has extensively been studied for its bulk and surface properties⁶ in view of numerous applications of the material but also as it is an excellent model system to study fundamental processes in a reducible oxide and specifically the interplay between surface properties and defects present at the surface and in the bulk of the crystal.^{6,7} The most commonly studied surface is the (110) surface of rutile titania exhibiting a characteristic row structure of bridging oxygens in its energetically most favourable unreconstructed state.⁸ Despite this principal simplicity, a clean, stoichiometric surface is not straightforward to be obtained. The surface cleaned by usual sputter procedures in the ultra-high vacuum (UHV) is highly reactive and upon annealing and exposing it to even small amounts of typical components of a residual gas, like oxygen, hydrogen or water, invokes most complicated surface chemical processes.^{9,10} This allows the preparation of the surface in distinctly different states characterized by surface stoichiometry and defect population where some of the states are stable in a UHV environment, others metastable due to their high reactivity towards components from the residual gas. Despite the popularity of this surface, not much is known about the work function of TiO₂(110). The nominal value for the clean, stoichiometric surface that has been reported to be in the range of 5.3–5.8 eV critically depends on the concentration of oxygen vacancies unavoidably generated during the preparation procedure.¹¹

Here, we systematically investigate the work function of four well defined and well characterized states of the unreconstructed TiO₂(110) surface as measured by metastable impact electron spectroscopy (MIES) and relate results to electron emission from band gap states measured with ultraviolet photoelectron spectroscopy (UPS). MIES is an electron spectroscopy technique that is specifically well suited for work function studies as it assures a high yield of secondary electrons for a minimum of excitation in the bulk of the material.¹² We find that a specific value for the work function is reproducibly associated with each of the surface states and that the work function smoothly moves from one value to the other, when

Fachbereich Physik, Universität Osnabrück, 49069 Osnabrück, Germany. E-mail: aborodin@uos.de, reichling@uos.de; Fax: +49 541 969-12264; Tel: +49 541 969-2264

transforming states into each other. We further find for some states that there is a weak but significant emission of electrons with energies below the threshold defined by the work function that is related to an emission peak found in the band gap region. We interpret this emission as originating from near-surface Ti^{3+} ion states localised near surface vacancies or hydroxyl defects as well as from near-surface interstitial Ti^{3+} ions. This allows us to establish a simple method for an unambiguous identification of the surface state solely based on a measurement of the work function and electron emission characteristics in the low energy cut-off region.

Measurements are performed in a UHV system equipped with a turbomolecular pump, a Ti-sublimator and a liquid nitrogen cooled cryo trap to maintain a base pressure of 7×10^{-11} mbar. Operating the cryo trap is important as this allows us to reduce the level of surface contamination to an absolute minimum. The homebuilt combined UPS/MIES source is in its construction and use similar to the one described in ref. 13. Metastable He^* atoms are generated in a cold cathode helium gas discharge and amplified in a second discharge. Metastable He^* atoms in the 2^3S state ($E_{\text{exc}} = 19.82$ eV) are mainly produced while a fraction of about 12% of atoms in the 2^1S state ($E_{\text{exc}} = 20.42$ eV) inevitably present in the atom beam undergoes the singlet–triplet conversion close to the surface¹² but does not affect the spectra. Furthermore, a strong flux of ultraviolet photons from the HeI resonance line ($h\nu = 21.22$ eV) is generated in the discharge that is used for UPS measurements. To separate MIES and UPS signals, the He^* beam is modulated with a frequency of 2000 Hz by a rotating chopper blade. Synchronizing the electron emission signal to a phase shifted signal from the chopper allows a time-of-flight selection facilitating the measurement of MIES and UPS HeI electron emission spectra quasi-simultaneously. The $\text{He}^*/$ photon beam impinges on the sample at an angle of 45° to its surface. Electrons emitted from the surface are collected perpendicular to the surface and energetically separated by a hemispherical electron analyser (PHOIBOS 100, SPECS GmbH, Berlin, Germany). To precisely resolve the low-energy cut-off in the electron spectra and to avoid possible irregularities of the analyser transmission function for electrons with low kinetic energies, the sample is biased by -15.00 V. For all spectra presented here, the kinetic energy scale is corrected for this bias voltage and also for the analyser work function, so that the low energy cut-off energy E_ϕ directly yields the sample work function ϕ . The cut-off energy E_ϕ is determined from electron emission spectra by linearly extrapolating the yield curve and determining the point of intersection with the zero yield axis. For a well-defined class of measurements representing specific surface states, we additionally observe a small but significant yield of electrons below E_ϕ . This feature as well as the value for the work function is perfectly reproducible by repetitive preparation of the same surface state evidencing that both are intrinsic properties of the respective surface state and not the result of an inhomogeneous surface preparation or other artefacts.

The (110) face of a $10 \times 10 \times 0.5$ mm TiO_2 crystal (highest available purity, MTI Corporation, Richmond, USA) is prepared by repeated sputter–annealing cycles described in detail in ref. 10. Briefly, sputtering for about 15 min by Ar^+

ions with an energy of 1 keV is followed by annealing at about 800–850 K for several minutes. To avoid excessive formation of defects in the bulk crystal, the temperature is never increased above this limit. The sample temperature is measured by a thermocouple (K-type) in contact with the sample holder close to the TiO_2 crystal. The initial preparation of the TiO_2 crystal consists of about 40 sputter–annealing cycles and before each experiment, the crystal surface is refreshed by at least one sputter–annealing cycle. In light of the high reactivity of the as-prepared TiO_2 surface, we minimized the time between preparation and measurements. Practically, it is possible to start collecting spectra a couple of minutes after flashing when the crystal is still at temperatures between 650 and 700 K. This procedure produces the reduced surface that is stoichiometric except for a concentration of typically 6 to 9% of vacancies statistically distributed over sites in the bridging oxygen rows of the unreconstructed $\text{TiO}_2(110)$ surface.^{9,10} Following a notation introduced in ref. 14, a surface prepared in this way will further on be denoted by $r\text{-TiO}_2$ and is the starting point for all other preparations. Such a surface can reproducibly be prepared on the same crystal many times, however, desorption of oxygen from the surface and diffusion of Ti^{3+} ions into the bulk result in a progressive reduction of the sample.^{15,16} When the number of such preparations exceeds a critical value, the bulk is so much reduced that an unreconstructed surface cannot be prepared anymore but other types of reconstructions appear.^{17,18} A crystal reaching this point in its sample history¹⁰ is discarded for further measurements in the context of the present work.

The preparation of the other three states of the surface investigated here is described in the following. When the freshly prepared $r\text{-TiO}_2$ surface is kept under UHV conditions, the progressive reaction of the surface with water from the residual gas can be observed as a systematic change in the UPS/MIES spectra; eventually a fully hydroxylated surface is yielded.¹⁰ We prepare the hydroxylated surface faster by exposing the $r\text{-TiO}_2$ surface kept at room temperature to 1–2 L of water introduced into the vacuum chamber while maintaining a water partial pressure of 2×10^{-9} mbar. It is well known that water molecules dissociate at oxygen vacancies and the vacancies are filled by an $\text{O}_{\text{br}}\text{H}$ complex while the excessive hydrogen atom forms an identical $\text{O}_{\text{br}}\text{H}$ complex with a neighbouring O_{br} so that effectively double hydroxyl groups are formed. Subsequent reaction of these species with water results in a splitting of double hydroxyls and a transfer of protons to a neighbouring oxygen row so that eventually the surface is covered with randomly distributed single hydroxyls in a density that is twice the density of the initially present vacancies.¹⁹ A surface prepared in this way will further on be denoted by $h\text{-TiO}_2$. Exposing the hydroxylated surface to molecular oxygen results in a further reaction yielding water desorbing and oxygen adatoms.^{9,10} We produce such a stoichiometric but oxygen covered surface by exposing the sample kept at room temperature to 0.4–2 L of oxygen with subsequent annealing at 450 K. A surface prepared in this way will further on be denoted by $\alpha x\text{-TiO}_2$. Oxygen exposure at elevated temperatures results in a similar process, however, water and oxygen are desorbed yielding a quasi-stoichiometric surface.²⁰ We produce this surface state by exposing the $r\text{-TiO}_2$ surface

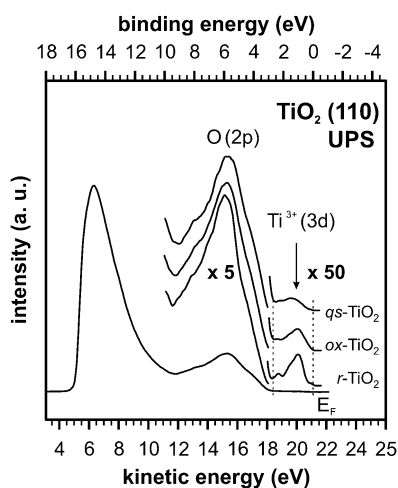


Fig. 1 UPS spectrum of the $\text{TiO}_2(110)$ surface in the $r\text{-TiO}_2$ state combined with band gap emission spectra for the $h\text{-TiO}_2$, $ox\text{-TiO}_2$ and $qs\text{-TiO}_2$ states. Respective curves are shifted vertically by an offset for clarity.

heated to 600 K to molecular oxygen introduced into the vacuum chamber while maintaining an oxygen partial pressure of 5×10^{-7} mbar for 10 to 15 min. A surface prepared in this way will further on be denoted by $qs\text{-TiO}_2$.

Fig. 1 and 2 show typical UPS and MIES spectra for the $r\text{-TiO}_2$ surface state. In Fig. 1, additionally magnified UPS spectral features from the band gap regions for the $r\text{-TiO}_2$, $ox\text{-TiO}_2$ and $qs\text{-TiO}_2$ surface states are displayed. The UPS spectrum for $r\text{-TiO}_2$ is similar to spectra published in the literature for reduced $\text{TiO}_2(110)$.^{21,22} The major feature is a peak of the O(2p) emission at a binding energy of -5.5 eV. The energetic distance between the Fermi level and the O(2p) top valence band edge is $E_{\text{VB}} = -3.0$ eV. Assuming that rutile TiO_2 has a band gap of $\Delta E_{\text{gap}} = 3.0$ eV,²³ we conclude that the Fermi level coincides with the bottom of the conduction band. The work function is found to be $\phi = 5.2$ eV. Note that this value and values of the work function for other surface states may be shifted by up to 0.2 eV by minute amounts of contaminants that are present if the cryo trap is not operated. The small peak at a binding energy of -0.9 eV is associated with $\text{Ti}^{3+}(3d)$ states from ions exposed at vacancy sites but also Ti^{3+} interstitial ions present in the near surface bulk.^{14,21} For $r\text{-TiO}_2$, the relative height of the $\text{Ti}^{3+}(3d)$ peak is estimated to be 1.5% of the O(2p) peak intensity.

The MIES spectrum displayed in Fig. 2 reveals neither a strong signal of the O(2p) emission nor of the $\text{Ti}^{3+}(3d)$ emission at energies corresponding to the respective peaks in the UPS spectrum in accordance with previous MIES studies on reduced crystals that also revealed an unexpectedly low height of the O(2p) peak.²⁴ From the published experimental evidence together with the results presented here, we conclude that on $\text{TiO}_2(110)$, the Auger neutralization (AN) process resulting in a smearing out of spectral features clearly dominates over the Auger deexcitation (AD) process that would reproduce the surface density of states (SDOS).¹² There are two electrons participating in the AN process, one from O(2p) and the other from either the O(2p) or the $\text{Ti}^{3+}(3d)$ state. In Fig. 2, we specify the expected energy ranges for electrons from both of

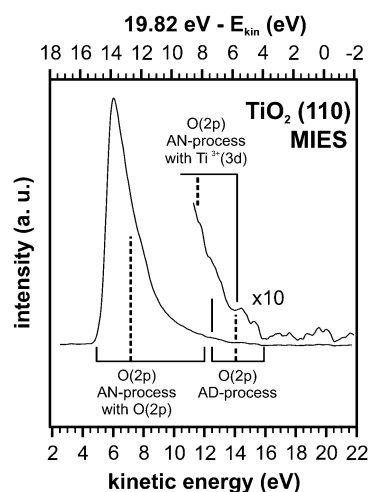


Fig. 2 MIES spectrum of the $\text{TiO}_2(110)$ surface in the $r\text{-TiO}_2$ state. The square brackets denote energy regions where electrons resulting from Auger detachment (AD) and Auger neutralisation (AN) processes are spread out.

these AN processes and the small feature from the O(2p) AD process.^{12,25,26} The superposition of all contributions yields a rather structureless spectrum sharply peaking towards E_{ϕ} . The work function derived from the MIES spectrum has, of course, precisely the same value as the one derived from the UPS spectrum.

We now focus entirely on the low energy cut-off region in the MIES spectra defining the energetic position E_{ϕ} of the work function ϕ . The cut-off energy is very well defined as MIES produces a high yield of both, secondary electrons and low energy electrons from AN processes contributing to the low energy peak. For the stoichiometric $\text{TiO}_2(110)$ surface, the electronegative oxygen will accumulate a negative charge in the surface layer yielding a high value for the work function that has been claimed to be 5.3–5.5 eV.¹¹ When oxygen is removed by the formation of bridging oxygen vacancies and the $r\text{-TiO}_2$ state is formed, the equilibrium defining the dipole layer will change and the work function is expected to decrease to a smaller value that is found to be 5.2 eV in our experiments. This value is perfectly reproducible for preparations yielding an estimated vacancy concentration in the range of 6 to 9%. A careful analysis in the cut-off region of the $r\text{-TiO}_2$ spectrum as shown in Fig. 3 and 4, however, reveals that there is a small fraction of electrons for which a smaller work function appears to be effective. The emission of such electrons is marked by the hatched area. We interpret this emission as resulting from electrons escaping the crystal *via* localized $\text{Ti}^{3+}(3d)$ states located near surface vacancies as well as $\text{Ti}^{3+}(3d)$ interstitial states as the emission is correlated with the band gap emission peak. The respective mechanisms will be discussed below in the context of the hydroxylated surface.

In a sequence of spectroscopy experiments, we study the transformation of the $r\text{-TiO}_2$ state into the $h\text{-TiO}_2$ state by progressive hydroxylation. Fig. 3 shows the respective changes in the cut-off region of the MIES spectra upon hydroxylation in UHV and upon water dosage. Spectrum I is the starting spectrum of the $r\text{-TiO}_2$ state. The work function decreases with an increasing number of surface vacancies converted to

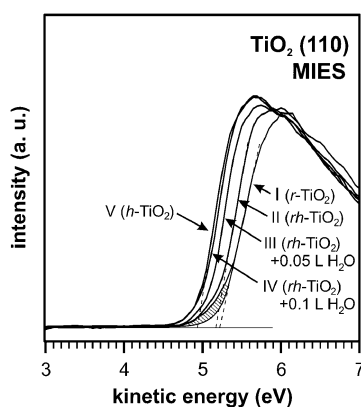


Fig. 3 Illustration of the transition from the *r*-TiO₂ surface state to the *h*-TiO₂ state by monitoring MIES secondary electron emission in the low energy cut-off region. (I) as prepared *r*-TiO₂ surface at 650 K, (II) partially hydroxylated *rh*-TiO₂ surface 10 minutes after preparation at 330 K, (III) and (IV) *rh*-TiO₂ surface exposed at RT to 0.05 L and 0.1 L of water, respectively; (V) fully hydroxylated *h*-TiO₂ surface after 10 L water exposure at 300 K. The hatched area indicates emission at energies below E_{ϕ} .

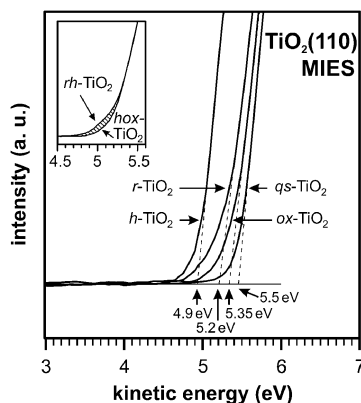


Fig. 4 Details of MIES secondary electron emission in the low energy cut-off region for the four well defined surface states. The inset demonstrates that *rh*-TiO₂ and *hox*-TiO₂ states having the same work function can be discriminated by their low energy emission characteristics. The hatched area indicates emission at energies below E_{ϕ} .

hydroxyls. In fact, this lowering of ϕ is the only noticeable change in MIES and UPS spectra during hydroxylation that up to here occurs solely due to water from the residual gas. A shift of the work function to a value of 4.9 eV is observed when the surface is exposed to 0.2 L water. The corresponding spectrum **V** establishes the saturation defining the *h*-TiO₂ state as we do not observe any change in the spectra after subsequent water exposure up to 10 L. It is important to note that even at a base pressure below 1×10^{-10} mbar, the work function instantly decreases when the temperature of the freshly prepared *r*-TiO₂ surface drops below 600 K as demonstrated by spectrum **II** in Fig. 3 that has been obtained without any deliberate water dosage. Spectrum **I** is collected at 650 K immediately after flashing while spectrum **II** reflects the work function 10 minutes later, after cooling the sample to room temperature. The progressively changing spectra obtained for water exposure with a dosage of 0.05 L and 0.1 L are represented by spectra **III** and **IV**. In accordance with claims in the literature,⁹ we find

that the effect of hydroxylation is reversible. Flashing the sample to a temperature of ~ 540 K restores the spectrum to that of *r*-TiO₂ in all details. This confirms the conclusion made on the basis of thermally programmed desorption measurements⁹ that at elevated temperatures the recombinative desorption of O_{br}H in the form $2\text{O}_{\text{br}}\text{H} \rightarrow \text{H}_2\text{O} + \text{V}_{\text{Obr}}$ takes place.

A specifically interesting feature of the MIES spectra is the emission that is observed for a limited number of electrons emitted with a kinetic energy below E_{ϕ} (hatched areas in Fig. 3 and 4) that is found for *r*-TiO₂, *h*-TiO₂ and spectra of a partially hydroxylated surface in between, denoted as *rh*-TiO₂. The low energy tail of all of these spectra adapts to the hatched stable shoulder of electron emission until the work function is so low that the shoulder contribution is only a minute addition to the much larger secondary electron yield. An important observation is that the intensity of this shoulder correlates with the Ti³⁺ (3d) peak observed in UPS for the same group of spectra. This emission does not depend on the degree of hydroxylation, however, the emission is much less pronounced for the *ox*-TiO₂ and *qs*-TiO₂ surface states. Combining the different pieces of experimental evidence, we conclude that the spectral feature found below ϕ is due to the emission of electrons from Ti³⁺ (3d) states related to vacancies and hydroxyls providing a local escape path with a lowered effective work function. As these states are preserved upon hydroxylation,^{10,27,28} the related electron emission yield is independent of the degree of hydroxylation but solely determined by the initial density of vacancies. It has been shown that the excess electron created by the formation of a vacancy localizes in the form of a small polaron primarily at a Ti³⁺ (3d) state in the vicinity of the surface defect, however, the details of localisation are under debate.^{27–29} We propose that the observed emission of secondary electrons below E_{ϕ} is intimately related to the origin of contrast formation in scanning tunnelling experiments on TiO₂(110). In standard STM experiments, the tunnel current is driven through unoccupied states having mainly Ti(3d) character^{10,20} which explains that titanium rows and, even more pronounced, vacancies and hydroxyls are imaged with a bright contrast as an apparent protrusion. Recently, however, filled state imaging of vacancies and hydroxyl defects by low temperature STM has shed new light on the question of electron localisation upon formation of vacancies and hydroxyl defects.²⁹ Experimental results combined with extensive theoretical modelling established convincing evidence that the excess electrons do not localise at single Ti³⁺ sites but the electron density is smeared out over several Ti sites next to the surface defects. We propose that upon photon or metastable atom induced excitation of the crystal, secondary electrons are emitted from these sites where the emitted electrons can quickly be replenished from the large reservoir of near surface secondary electrons. As the emitting state is fairly localised, a dynamic local equilibrium between electron emission and electron replenishment can be established and, apparently, the resulting local work function is smaller than the work function governed by the surface dipole layer in the rest of the crystal. This yet speculative model explains why the secondary electron emission below E_{ϕ} is observed for the surface decorated with vacancy defects, does not change upon hydroxylation of

the vacancies but vanishes for the oxidised and quasi-stoichiometric surface states as described below. However, rigorous analysis reveals that even for the *qs*-TiO₂, UPS emission from Ti³⁺ (3d) states does not vanish completely. In a similar manner the emission below E_{ϕ} in MIES is nearly completely absent for *ox*-TiO₂ and *qs*-TiO₂ for a crystal early in its sample history where the degree of bulk reduction, *i.e.* the concentration of Ti³⁺ interstitials, is small. This points to interstitials additionally contributing to the emission below E_{ϕ} that will be addressed by future investigations.

Exposing the fully hydroxylated surface to molecular oxygen at room temperature or at low temperature is expected to result in the *ox*-TiO₂ state that is a stoichiometric surface covered with oxygen ad-atoms in a density corresponding to the initially present number of hydroxyls. The related surface chemistry has been elucidated by STM,¹⁰ EELS,⁹ and TPD⁹ measurements revealing a reaction between O₂ and two hydrogen atoms from neighbouring O_{br}H that yields a water molecule and an oxygen adatom on top of the bridging oxygen row. It has been claimed that the same surface state can be formed by exposure of the reduced surface to oxygen at room temperature⁹ where O₂ dissociates at vacancies. To test this hypothesis, we expose both the hydroxylated and the reduced surface to 0.4 L of oxygen. The work function of *h*-TiO₂ after oxidation restores the value close to that for *rh*-TiO₂, which is probably affected by molecular water present on the surface. Such a surface is referred to as *hox*-TiO₂. Heating this surface to a temperature of up to 450–470 K presumably leads to water desorption and yields spectra identical to those for *r*-TiO₂ treated with 0.4 L of oxygen; this is the surface in its *ox*-TiO₂ state having a work function of 5.35 eV. Most importantly, for the *ox*-TiO₂ and *hox*-TiO₂ states we find a reduced emission below E_{ϕ} compared to spectra for the *r*-TiO₂, *h*-TiO₂ and *rh*-TiO₂ surface states. This allows for an unambiguous discrimination between *hox*-TiO₂ and *rh*-TiO₂ states by their signatures in the cut-off region even if their work functions are identical as it is demonstrated in the inset of Fig. 4. In complete agreement with the interpretation of the low kinetic energy emission resulting from localized Ti³⁺ (3d) states, the Ti³⁺ (3d) peak in UPS spectra decreases and the residual emission is attributed to Ti³⁺ interstitials. Once prepared in the *ox*-TiO₂ state, the surface appears to be stable in UHV as we do not observe any noticeable changes in the spectra even for prolonged exposure of the surface to the residual gas.

Aiming at the preparation of fully stoichiometric TiO₂(110), we expose the surface in the *r*-TiO₂ state to oxygen while maintaining a temperature of ~600 K. We denote the resulting surface state as quasi-stoichiometric, *qs*-TiO₂, since the MIES and UPS spectra reveal all features we would expect from a fully stoichiometric surface except for a small emission below E_{ϕ} as evident from Fig. 4. While in UPS, the O2(p) emission is fully developed, the Ti³⁺ (3d) emission in the band gap region is very small but still discernible from the background (see Fig. 1). The work function is found to be 5.5 eV which is close to the most reliable value that has been reported for a TiO₂(110) surface that can be expected to be of similar quality.¹¹ The low energy tail is qualitatively the same as for the defective surfaces but from a comparison of the areas under the spectra in the tail area, we can roughly estimate that

the emission intensity is by a factor of six smaller. We note that the TiO₂(110) surface in the *qs*-TiO₂ state is quite resistant against degradation under UHV conditions. Once prepared, the work function gradually decreases to a value of 5.1 eV in UHV, however, even when *qs*-TiO₂ is exposed to 10 L of water, the work function will not decrease to the work function of the hydroxylated surface (4.9 eV). From these findings we conclude that the *qs*-TiO₂ state represents a surface that may have a rosette structure overlayer³⁰ but is stoichiometric except for a small number of residual hydroxyl defects. The slow degradation presumably stems from the interplay between the quasi-stoichiometric surface and the reservoir of Ti³⁺ interstitials in the bulk. At the high temperatures required to prepare the quasi-stoichiometric surface, the interstitials are likely to diffuse to the surface and invoke surface chemistry like the formation of TiO_x patches³¹ or non-stoichiometric surface reconstructions when interacting with oxygen.¹⁷

Summarizing our findings, we investigate four well defined states of the unreconstructed TiO₂(110) surface that we can transform into each other in a controlled way and unambiguously identify by their work function and secondary electron emission characteristics in the low energy cut-off region. These surface states, their work functions and the pathways of transforming one into the other are summarized in the scheme presented in Fig. 5. The starting point of any well prepared TiO₂(110) surface is the *r*-TiO₂ state having a work function of 5.2 eV and a significant electron emission tail below E_{ϕ} . This tail is attributed to emission from Ti³⁺ (3d) states localized around vacancies but also Ti³⁺ interstitials. The *r*-TiO₂ surface state is, however, not stable but most susceptible to reaction with water and will inevitably be converted to the hydroxylated *h*-TiO₂ state even under the conditions of an ultra-high vacuum. The surface in its fully hydroxylated *h*-TiO₂ state has a work function of 4.9 eV, and this state as well as all transition states between *r*-TiO₂ and *h*-TiO₂ also exhibit band gap emission from localized Ti³⁺ (3d) states and electron emission below E_{ϕ} . The transformation to the *h*-TiO₂ state is reversible, *i.e.* by annealing the sample in UHV one can fully re-establish the *r*-TiO₂ state. Exposing the surface in its *h*-TiO₂ state to molecular oxygen yields the *ox*-TiO₂ state that is a stoichiometric surface with oxygen ad-atoms exhibiting a work function of 5.35 eV but no emission below E_{ϕ} . The *ox*-TiO₂ state is found to be stable under UHV conditions. An alternative way of creating the *ox*-TiO₂ state is by exposing the surface in its *r*-TiO₂ state to oxygen at room temperature. However, exposing the surface in its *r*-TiO₂ state to oxygen at

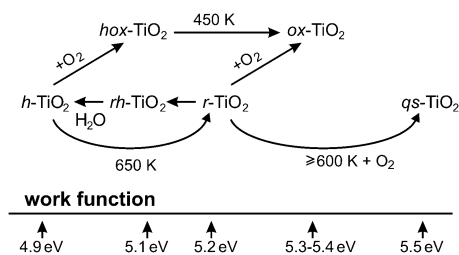


Fig. 5 Schematic overview of the four well defined TiO₂(110) surface states, their work functions and preparation steps for a transformation of one state into another.

elevated temperatures produces the qs -TiO₂ that is a stoichiometric surface with a very small number of defects. This surface has the highest work function, namely 5.5 eV and does exhibit only minute band gap emission and minute secondary electron emission below E_{ϕ} .

A major finding of this and related work is that it is most difficult to prepare and maintain non-reconstructed, stoichiometric TiO₂(110). The best we could obtain is a quasi-stoichiometric surface that is metastable in the sense that it slowly degrades in the residual gas. Both of the stable states, namely h -TiO₂ and ox -TiO₂, represent surfaces covered by defects, namely protons or oxygen atoms in a density that is determined by the density of vacancies of the initially prepared reduced surface state. The main result of our work is, however, that all of the well-defined surface states can be unambiguously identified by a measurement of their work function and the low energy electron emission tail. Any deviation from the specified features is a clear indication of incomplete preparation or contamination. While the physics behind the shift in work function remains to be elucidated in detail, the rather simple methodology introduced here provides a new tool for the characterisation and control of well-defined states of the TiO₂(110) surface.

Acknowledgements

The authors are grateful to H.-P. Steinrück and A. L. Shluger for a discussion of the work on the occasion of the final meeting of the COST D41 action. Support from the COST action is gratefully acknowledged. We also acknowledge stimulating discussions with S. Wendt.

References

- 1 J. Hölzl and F. K. Schulte, *Solid Surface Physics*, vol. 85, Springer Tracts in Modern Physics Springer, Berlin/Heidelberg, 1979.
- 2 H. Ishida and K. Terakura, *Phys. Rev. B: Condens. Matter*, 1987, **36**, 4510.
- 3 H. Ishii, K. Sugiyama, E. Ito and K. Seki, *Adv. Mater.*, 1999, **11**, 972.
- 4 S. Trasatti, *J. Chem. Soc., Faraday Trans. 1*, 1972, **68**, 229.
- 5 E. L. Bruner, N. Koch, A. R. Span, S. L. Bernasek, A. Kahn and J. Schwartz, *J. Am. Chem. Soc.*, 2002, **124**, 3192.
- 6 V. E. Henrich and P. A. Cox, *The surface science of metal oxides*, Cambridge University Press, Cambridge, 1996.
- 7 U. Diebold, *Surf. Sci. Rep.*, 2003, **48**, 53.
- 8 U. Diebold, *Appl. Phys. A: Mater. Sci. Process.*, 2003, **76**, 681.
- 9 M. A. Henderson, W. S. Epling, C. H. F. Peden and C. L. Perkins, *J. Phys. Chem. B*, 2003, **107**, 534.
- 10 S. Wendt, R. Schaub, J. Matthiesen, E. K. Vestergaard, E. Wahlström, M. D. Rasmussen, P. Thostrup, L. M. Molina, E. Lægsgaard, I. Stensgaard, B. Hammer and F. Besenbacher, *Surf. Sci.*, 2005, **598**, 226.
- 11 K. Onda, B. Li and H. Petek, *Phys. Rev. B: Condens. Matter Mater. Phys.*, 2004, **70**, 11.
- 12 Y. Harada, S. Masuda and H. Ozaki, *Chem. Rev.*, 1997, **97**, 1897.
- 13 W. Maus-Friedrichs, M. Wehrhahn, S. Dieckhoff and V. Kempter, *Surf. Sci.*, 1990, **237**, 257.
- 14 S. Wendt, P. T. Sprunger, E. Lira, G. K. H. Madsen, Z. S. Li, J. Ø. Hansen, J. Matthiesen, A. Blekinge-Rasmussen, E. Lægsgaard, B. Hammer and F. Besenbacher, *Science*, 2008, **320**, 1755.
- 15 R. A. Bennett, P. Stone, N. J. Price and M. Bowker, *Phys. Rev. Lett.*, 1999, **82**, 3831.
- 16 H. Nörenberg and G. A. D. Briggs, *Surf. Sci.*, 1998, **402–404**, 738.
- 17 M. Bowker and R. A. Bennett, *J. Phys.: Condens. Matter*, 2009, **21**, 474224.
- 18 H. H. Pieper, K. Venkataramani, S. Torbrügge, S. Bahr, J. V. Lauritsen, F. Besenbacher, A. Kühnle and M. Reichling, *Phys. Chem. Chem. Phys.*, 2010, **12**, 12436.
- 19 S. Wendt, J. Matthiesen, R. Schaub, E. K. Vestergaard, E. Lægsgaard, F. Besenbacher and B. Hammer, *Phys. Rev. Lett.*, 2006, **96**, 066107.
- 20 U. Diebold, J. F. Anderson, K.-O. Ng and D. Vanderbilt, *Phys. Rev. Lett.*, 1996, **77**, 1322.
- 21 S. Kodaira, Y. Sakisaka, T. Maruyama, Y. Haruyama, Y. Aiura and H. Kato, *Solid State Commun.*, 1994, **89**, 9.
- 22 R. L. Kurtz, R. Stockbauer, T. E. Madey, E. Román and J. L. de Segovia, *Surf. Sci.*, 1989, **218**, 178.
- 23 O. Diwald, T. L. Thompson, T. Zubkov, E. G. Goralski, S. D. Walck and J. T. Yates, *J. Phys. Chem. B*, 2004, **108**, 6004.
- 24 M. Brause, S. Skordas and V. Kempter, *Surf. Sci.*, 2000, **445**, 224.
- 25 W. Maus-Friedrichs, M. Frerichs, A. Gunhold, S. Krischok, V. Kempter and G. Bihlmayer, *Surf. Sci.*, 2002, **515**, 499.
- 26 A. Gunhold, L. Beuermann, K. Gomann, G. Borchardt, V. Kempter, W. Maus-Friedrichs, S. Piskunov, E. A. Kotomin and S. Dorfman, *Surf. Interface Anal.*, 2003, **35**, 998.
- 27 N. A. Deskins, R. Rousseau and M. Dupuis, *J. Phys. Chem. C*, 2009, **113**, 14583.
- 28 C. Di Valentin, G. Pacchioni and A. Selloni, *Phys. Rev. Lett.*, 2006, **97**, 1666803.
- 29 T. Minato, Y. Sainoo, Y. Kim, H. S. Kato, K. Aika, M. Kawai, J. Zhao, H. Petek, T. Huang, W. He, B. Wang, Z. Wang, Y. Zhao, J. L. Yang and J. G. Hou, *J. Chem. Phys.*, 2009, **130**, 124502.
- 30 M. Li, W. Hebenstreit, U. Diebold, M. A. Henderson and D. R. Jennison, *Faraday Discuss.*, 1999, **114**, 245.
- 31 Z. Zhang, J. Lee, J. T. Yates, R. Bechstein, E. Lira, J. Ø. Hansen, S. Wendt and F. Besenbacher, *J. Phys. Chem. C*, 2010, **114**, 3059.